Journal of Chromatography B, 923–924 (2013) 54–64

Contents lists available at SciVerse ScienceDirect

Journal of Chromatography B

journal homepage: www.elsevier.com/locate/chromb

Analysis of iridoid glucosides from *Paederia scandens* using HPLC–ESI-MS/MS

Zhi-Jun Wu[a,*], Jian-Hua Wang[b], Dong-Mei Fang[a], Guo-Lin Zhang[a]

[a] *Chengdu Institute of Biology, Chinese Academy of Sciences, Chengdu 610041, China*
[b] *College of Bioengineering, Chongqing University, Chongqing 400044, China*

ARTICLE INFO

Article history:
Received 11 June 2012
Accepted 23 January 2013
Available online 4 February 2013

Key words:
Iridoid glycosides
Electrospray
Natural product
Paederia scandens
Fragmentation
HPLC–ESI-MS/MS

ABSTRACT

Iridoid glycosides are an important class of natural products and have many biological activities. Iridoid glucosides in an extract of the plant species *Paederia scandens* were investigated using reversed-phase high performance liquid chromatography and electrospray quadrupole time-of-flight-type tandem mass spectrometry. The elemental composition of most of the compounds was determined by accurate mass and relative isotopic abundance (RIA) measurements. In positive ion mode, the fragmentation of $[M+NH_4]^+$ precursor ions was carried out using low energy collision-induced electrospray ionization tandem spectrometry. The neutral losses of NH_3, H_2O, Glc, and the side chain of the iridoid moiety were the main fragmentation patterns observed. For simple iridoid glycosides, the main differences were related to the side chains. Fragmentation of the $[M-H]^-$ precursor ions was achieved for the compounds possibly having phenolic acid group. The connection order of the iridoid, sugar, and phenolic acid moieties, and the linkage of the 6-OH group of the sugar to the phenolic acid were unambiguously confirmed using a combination of MS/MS spectra in both positive and negative ion modes, and our previous work. For some trace dimeric iridoid glucosides, the connection order between the asperuloside and paederoside moieties was determined by the characteristic product ions; this was supported by D-labeling experiments. A total of 24 iridoid glucosides, including 14 new species, were identified or tentatively characterized based on exact mass, RIA values, tandem mass spectra, and D-labeling experiments.

1. Introduction

The vine *Paederia scandens* is widely distributed in India, Japan, the Philippines and the USA [1]. It has long been used in India, China and Vietnam for the treatment of toothache, chest pain, piles, inflammation of the spleen, rheumatic arthritis, and bacillary dysentery [2,3]. Iridoid glycosides have been isolated as major compounds from the stem and root of *P. scandens* [4–9], and found to have antiviral, antitumor, anti-inflammatory, antinociceptive and antimicrobial activities [2,10–12].

Structural characterization of a natural product is the key to study its bioactivity. However, characterization has always been a challenge, especially for those compounds and their metabolites that occur in trace amounts. Nuclear magnetic resonance (NMR) spectroscopy offers detailed structural information, but requires laborious purification of the compounds, and some oligomers consisting of structurally similar monomers are difficult to identify by NMR [13–15].

Mass spectrometry (MS) is an important physicochemical technique for the identification of trace natural products in extracts, particularly because of its rapidity, and sensitivity, and the very small quantities of sample required. A number of iridoid glucosides have been studied by electrospray ionization mass spectrometry (ESI-MS/MS) [16–18]. In negative ion mode, the formate adduct ion $[M+HCOO]^-$ is a diagnostic ion for distinguishing iridoid glucosides that have a methyl ester, lactone, or carboxyl group, when formic acid is used as an additive [18]. Zhou et al. reported the fragmentation pathways of the $[M+Na]^+$ precursor ions for four sulfur-containing iridoid glucosides [19]. Relatively high collision-induced energy (40 eV) for $[M+Na]^+$ precursor ions reduces the ion intensity markedly, making these ions unsuitable as precursors, particularly for natural products present in trace amounts.

The chemical basis of traditional Chinese medicine has been widely investigated. Several of the main components have been identified by high resolution mass spectrometry (HRMS), and can be used as standard samples, avoiding the necessary for the time-consuming and repetitious processes of purifying these compounds. In this study, high performance liquid chromatography and electrospray quadrupole time-of-flight-type tandem mass spectrometry (HPLC–ESI-QTOF) were used for the phytochemical analysis of an extract of *P. scandens*. A series of iridoid glucosides,

* Corresponding author. Tel.: +86 28 82890717; fax: +86 28 82890513.
E-mail address: wuzj@cib.ac.cn (Z.-J. Wu).

1570-0232/$ – see front matter © 2013 Elsevier B.V. All rights reserved.
http://dx.doi.org/10.1016/j.jchromb.2013.01.032

including previously unknown trace dimeric iridoid glucosides, was identified or tentatively characterized based on exact masses, relative isotopic abundance (RIA) values, tandem mass spectra, and D-labeling experiments.

2. Experimental

2.1. Chemicals

HPLC-grade acetonitrile, thrice deionized water, ammonium acetate, deuterium oxide, and a mass calibration standard for use in the analyses were obtained from Fisher Scientific (Pittsburgh, PA, USA), Fluka (Switzerland), Haihong (Chengdu, China), Guoyao (Chengdu, China), Merck (Andover, MA, USA) and Agilent Technologies (Palo Alto, CA, USA), respectively. The stems of *P. scandens* were collected in June 2011 from Anyue, Sichuan province, China. Extracts were prepared in 95% ethanol, petroleum ether, ethyl acetate, and n-butanol, obtained from Bodi Corp. (Tianjin, China).

2.2. Extract preparation

The stems were soaked with 95% ethanol for 24 h at room temperature, and the solvent was evaporated under reduced pressure. The resulting dry extract was suspended in water, which was fractionated sequentially with petroleum ether, ethyl acetate, and n-butanol. The solution of n-butanol was evaporated and the dry extract was dissolved in methanol, and filtered (0.45 μm membrane filter) prior to analysis by HPLC–MS.

2.3. Chromatography

We used an Agilent 1100 series HPLC equipped with a quaternary pump, a diode-array detector, an autosampler, and a thermostatted column compartment. The samples were separated using a Kinetex C18 column (2.6 μm, 2.1 mm × 100 mm) from Phenomenex (Torrance, CA, USA). The mobile phase consisted of (B) acetonitrile and (A) water containing 0.5% ammonium acetate. An adduct of ammonium acetate in water can improve the MS signal and inhibit peak tails. The flow rate was 0.2 ml/min, the column temperature was 25 °C, and the total run time was 35 min. An isocratic mode of 92% phase A was applied for 5 min, following which a linear gradient from 8% to 80% phase B was applied over the next 30 min. The D-labeling experiments were carried out using deuterium oxide instead of water as the mobile phase (A).

2.4. Mass spectrometry

MS experiments were performed using a Bruker micrOTOF-Q mass spectrometer (Bremen, Germany). The mass resolution was 10,000 FWHM at 922 μ. Helium was used as the collision gas, and high-purity nitrogen was used as the nebulizer and dry gas at flow rates of 0.4 L/min and 8.0 L/min, respectively. The ESI source conditions were as follows: capillary V, −4500 V (positive), 4000 V (negative); end plate voltage, −4000 V (positive), 3500 V (negative); capillary exit voltage, 120 V; and dry gas temperature, 180 °C. The mass data were processed using Bruker Compass DataAnalysis 4.0 software.

2.5. Molecular formula analysis

A make-before-break (MBB) valve was installed between the HPLC and the MS to introduce the solution of mass calibration standards. Relative isotopic abundance (RIA) measurements of [M+1]/M and [M+2]/M provided important information on the number of C and S atoms in the corresponding molecular formula. The N rule and the loss of NH_3 (or sequential losses of NH_3 and H_2O) were used for determining the precursor $[M+NH_4]^+$ ions. The determination of the accurate masses of low mass product ions and conventional neutral losses can provide information on the number of C, H, O, and S atoms.

3. Results and discussion

3.1. Structural analysis of known compounds 1–4

The $[M+NH_4]^+$ ions for compounds **1**–**4** were detected in positive ion mode. The molecular formula of compound **1** was confirmed as $C_{18}H_{24}O_{12}S$, based on accurate mass and RIA measurements (Table 1). Compound **1** is paederosidic acid (**1**) (Fig. 1), and was the main compound in the extract of *P. scandens*. Compound **2** may

Table 1
Elemental constituents of $[M+NH_4]^+$ ions and RIA errors in MS spectra of iridoid glucosides.

Compound	Formula ($[M+NH_4]^+$)	Calculated (m/z)	Observed (m/z)	Error (ppm)	RIA_{error}[a] (%) (I_{M+1}/I_M)	RIA_{error} (%) (I_{M+2}/I_M)
Paederosidic acid (**1**)	$C_{18}H_{28}NO_{12}S$	482.1327	482.1331	−0.8	−4.3	−8.1
Paederoside (**2**)	$C_{18}H_{26}NO_{11}S$	464.1221	464.1245	−5.1	–	–
Asperulosidic acid (**3**)	$C_{18}H_{28}NO_{12}$	450.1606	450.1599	1.6	−2.5	−1.6
Asperuloside (**4**)	$C_{18}H_{26}NO_{11}$	432.1500	432.1501	−0.2	–	–
5	$C_{19}H_{30}NO_{12}$	464.1763	464.1755	1.7	3.0	0.6
6	$C_{20}H_{30}NO_{12}S$	508.1483	508.1510	−5.3	9.7	7.3
7	$C_{21}H_{34}NO_{12}$	492.2076	492.2054	4.5	0.8	–
Geniposidic acid (**8**)	$C_{16}H_{26}NO_{10}$	392.1551	392.1534	4.3	10.3	–
Deacetylasperulosidic acid (**9**)	$C_{16}H_{26}NO_{11}$	408.1500	408.1506	−1.5	–	–
Decatylasperuloside acid methyl ester (**10**)	$C_{17}H_{28}NO_{11}$	422.1657	422.1659	−0.5	5.6	–
11	$C_{16}H_{26}NO_{12}$	424.1450	424.1466	−3.8	–	–
12	$C_{24}H_{28}NO_{12}$	522.1606	522.1634	−5.4	–	–
13	$C_{25}H_{32}NO_{13}$	554.1868	554.1874	−1.1	−4.0	9.2
14	$C_{25}H_{32}NO_{14}$	570.1817	570.1807	1.8	−2.8	10.8
15	$C_{26}H_{34}NO_{14}$	584.1974	584.1973	0.2	0.6	–
16	$C_{24}H_{38}NO_{17}S$	644.1855	644.1858	−0.5	3.7	−1.3
17	$C_{24}H_{38}NO_{17}$	612.2134	612.2131	0.5	10.1	–
18	$C_{30}H_{40}NO_{17}$	686.2291	686.2301	−1.5	8.5	−10.1
19	$C_{36}H_{48}NO_{22}S_2$	910.2104	910.2117	−1.4	-6.8	−10.6
20	$C_{36}H_{48}NO_{22}S_2$	910.2104	910.2113	−1.0	-6.3	−8.1
21	$C_{36}H_{48}NO_{22}S$	878.2383	878.2399	−1.8	5.6	0.0
22	$C_{36}H_{48}NO_{22}S$	878.2383	878.2397	−1.6	3.6	−1.7
23	$C_{36}H_{48}NO_{22}S$	878.2383	878.2417	−3.9	–	–
24	$C_{36}H_{48}NO_{22}S$	878.2383	878.2413	−3.4	–	–

[a] RIA_{error} (%) = 100 × (RIA_{exp} − RIA_{theo})/RIA_{theo}.

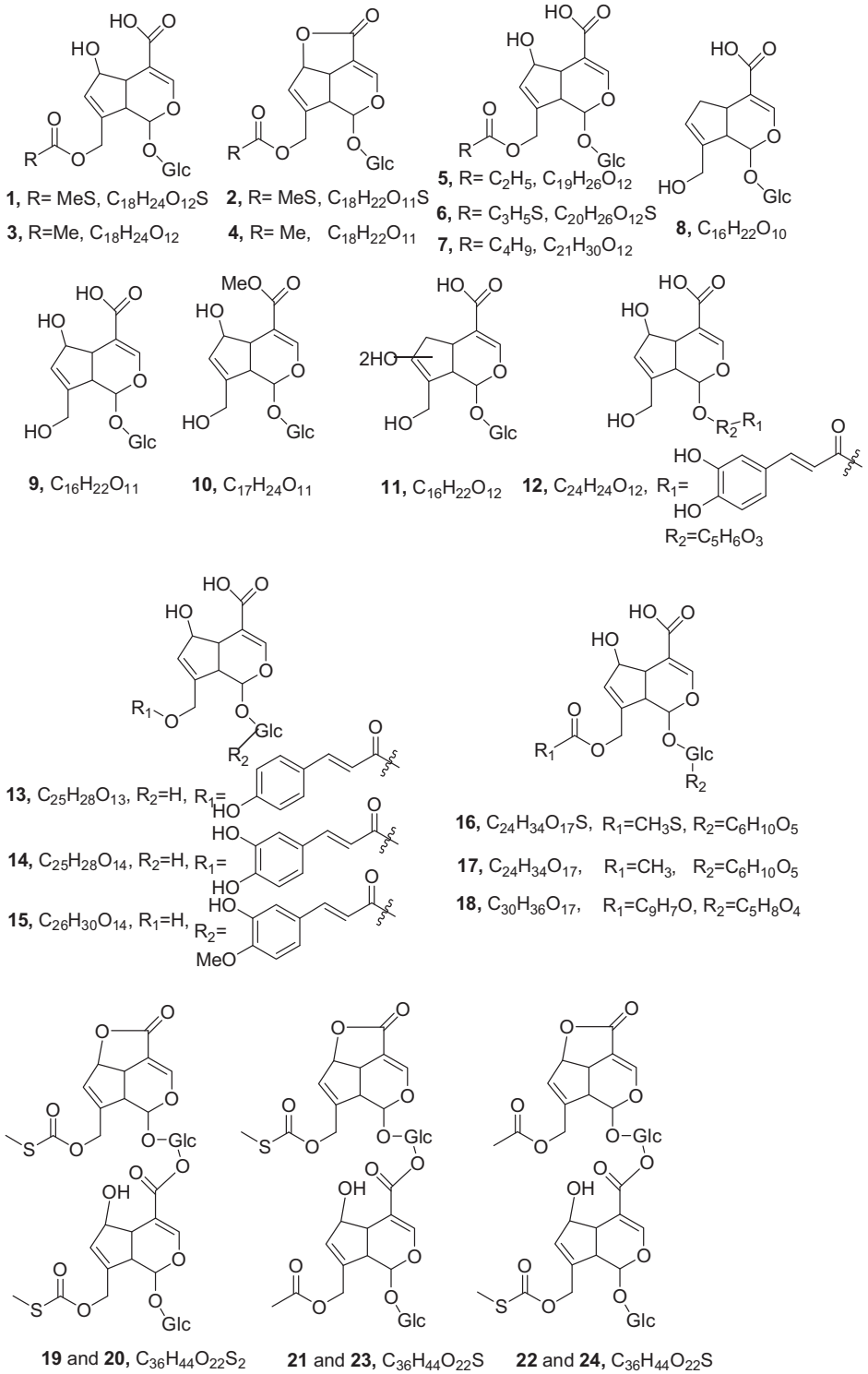

Fig. 1. Iridoid glucosides: paederosidic acid (**1**, *Mr* 464.0988); paederoside (**2**, *Mr* 446.0883); asperulosidic acid (**3**, *Mr* 432.1268); asperuloside (**4**, *Mr* 414.1162); compound **5**, (*Mr* 446.1424); compound **6**, (*Mr* 490.1145); compound **7**, (*Mr* 474.1737); geniposidic acid (**8**, *Mr* 374.1213); deacetylasperulosidic acid (**9**, *Mr* 390.1162); decatylasperuloside acid methyl ester (**10**, *Mr* 404.1319); compound **11**, (*Mr* 406.1111); compound **12**, (*Mr* 504.1268); compound **13**, (*Mr* 536.1530); compound **14**, (*Mr* 552.1479); compound **15**, (*Mr* 566.1636); compound **16**, (*Mr* 626.1517); compound **17**, (*Mr* 594.1796); compound **18**, (*Mr* 668.1952); compounds **19** and **20**, (*Mr* 892.1766); compound **21**–**24**, (*Mr* 860.2045). Compounds **5**–**7**, **12**–**18**, and **21**–**24** are novel compounds.

be paederoside (**2**), based on its molecular formula. ($C_{18}H_{22}O_{11}S$; Table 1). Product ion scans of the precursor $[M+NH_4]^+$ were recorded at *m*/*z* 482 and 464 for compounds **1** and **2** respectively. The fragmentation pathways of compounds **1** and **2** were proposed based on comparison of their tandem spectra. The loss of H_2O at *m*/*z* 482 for **1** occur readily and further formed the product ion at *m*/*z* 447 having a lactone structure, by the loss of a NH_3 molecule. The low mass product ions in the MS/MS spectra of **1** were formed by the neutral losses of Glc, H_2O, CH_3SCOOH, CO and HCOOH (individually or in combination) from *m*/*z* 447. The product ions at *m*/*z* 193, 175, 165 and 147 were likely characteristic ions of the iridoid moiety. Similar fragmentation pathways for **2** were observed.

The molecular formula of compounds **3** was confirmed as $C_{18}H_{24}O_{12}$, and the MS/MS spectrum of this compound was very similar to that of **1**. This indicates that the skeleton structure of **3** is the same as that of **1**, and the data suggested that the former may be asperulosidic acid (**3**) (Fig. 1 and Table 1). Compound **4** was putatively identified as asperuloside (**4**), based on the accurate mass determination and tandem MS spectra.

In negative ion mode, the deprotonated molecular ion $[M-H]^-$ of **1** was observed, and selected as the precursor ion for the product ion scan. Neutral losses of Glc, H_2O, CH_3SCOOH, CH_3SH and CO_2 comprised the main fragmentation patterns. The product ion at *m/z* 121 was produced by the retro Diels–Alder (RDA) reaction from *m/z* 191. For **2**, a high abundance $[M+CH_3COO]-$ ion was detected in negative ion mode, as reported previously [18]. It seemed that the $[M+CH_3COO]-$ ion was negligible when carboxyl was present. As in the positive ion mode, in negative ion mode, **3** and **4** had similar MS and MS/MS behaviors to compounds **1** and **2** respectively.

3.2. Structural analysis of compounds 5–7 with novel side chains

In positive ion mode, the accurate mass of $[M+NH_4]^+$ at *m/z* 464.1755 corresponded to the molecular formula $C_{19}H_{26}O_{12}$ (compound **5**). The corresponding MS/MS spectrum was very similar to that of **1** and **3** (Fig. 2(a) and supporting information). Thus, compounds **1**, **3** and **5** had the same skeleton structure, the only difference being the side chain on the iridoid moiety. The neutral loss of $C_3H_6O_2$ from the product ion at *m/z* 267 indicated that the side chain on the iridoid moiety of **5** was propylene acyl rather than acyl, as occurred in **3**. The structure of compounds **6** and **7** was very similar to that of **1**, **3**, and **5** based on their MS/MS spectra (Fig. 2), with the difference being side chain. The molecular formulae of unknown side chain group of for compounds **6** and **7** were confirmed as C_3H_5 (cyclopropyl or allyl) and C_4H_9 (butyl), respectively. Compounds **5**–**7** are novel compounds.

3.3. Structural analysis of compounds 8–11 without side chains

For compound 8, the accurate mass of the $[M+NH_4]^+$ precursor ion at *m/z* 392.1534 provided the molecular formula $C_{16}H_{22}O_{10}$, and based on the MS/MS spectrum (Supporting Information and Fig. 3(a)) there are three possible structures (a–c) for this compound. The high abundance product ion detected at *m/z* 213 was derived from *m/z* 392 by sequential loss of NH_3 and Glc, which implied that structures (b) and (c) are more likely than structure (a). Analysis of **1** and **3** indicated that the product ion at *m/z* 213 should be negligible for structure (a). In negative ion mode, the precursor ion $[M+CH_3COO]-$ for **1** was not observed, but the precursor ion $[M-H]^-$ was in high abundance. This indicated that compound **8** is geniposidic acid (structure (c)). The MS/MS spectrum of $[M-H]-$ at *m/z* 373 is shown in Fig. 3(b) and this further supported the proposed structure (c).

The accurate mass of the $[M+NH_4]^+$ precursor ion at *m/z* 408.1506 gave the molecular formula $C_{16}H_{22}O_{11}$ for compound **9**. The MS/MS spectrum of $[M+NH_4]^+$ at *m/z* 408 is shown in Fig. 3c. The product ion at *m/z* 373, resulting from *m/z* 408 by sequential losses of a H_2O and a NH_3 molecule, produced the product ion at

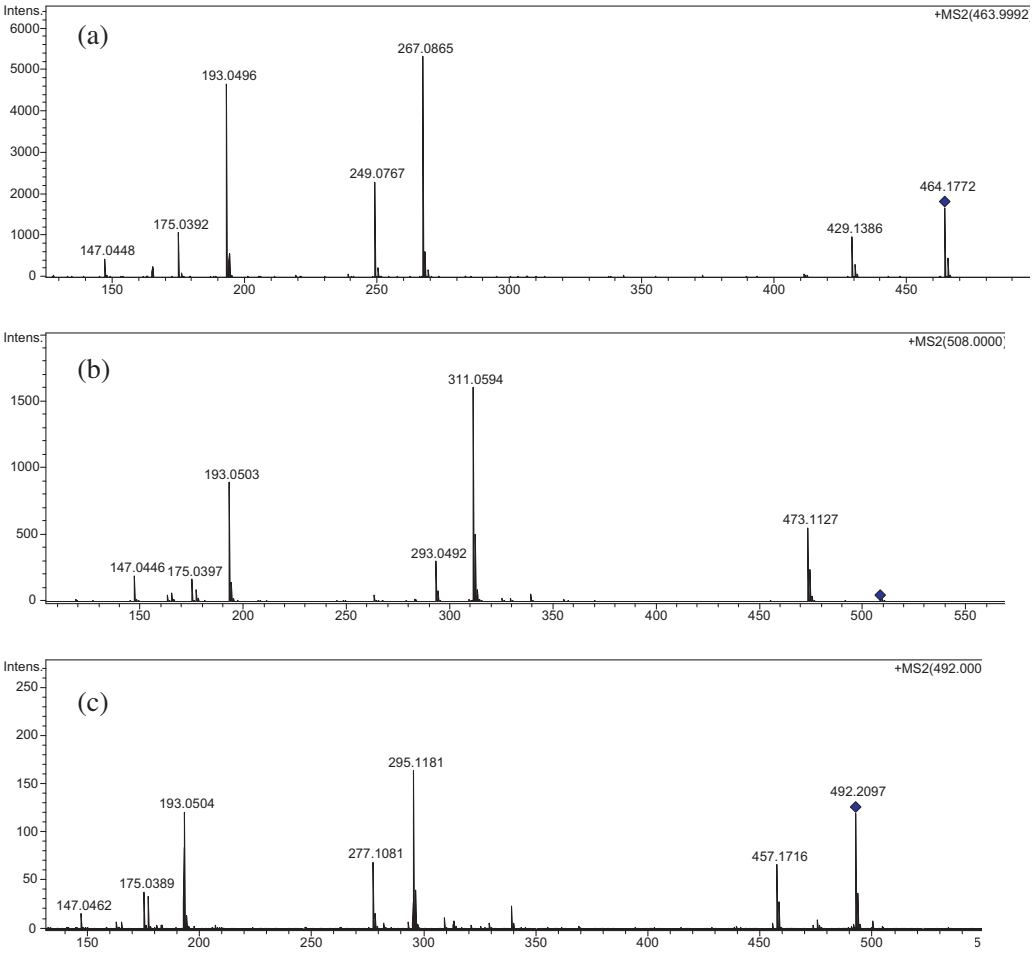

Fig. 2. Product ion scan of the selected precursor $[M+NH_4]^+$: (a) at *m/z* 464 for compound **5** (collision energy: 8 eV); (b) at *m/z* 508 for compound **6** (collision energy: 10 eV); and (c) at *m/z* 492 for compound **7** (collision energy: 8 eV).

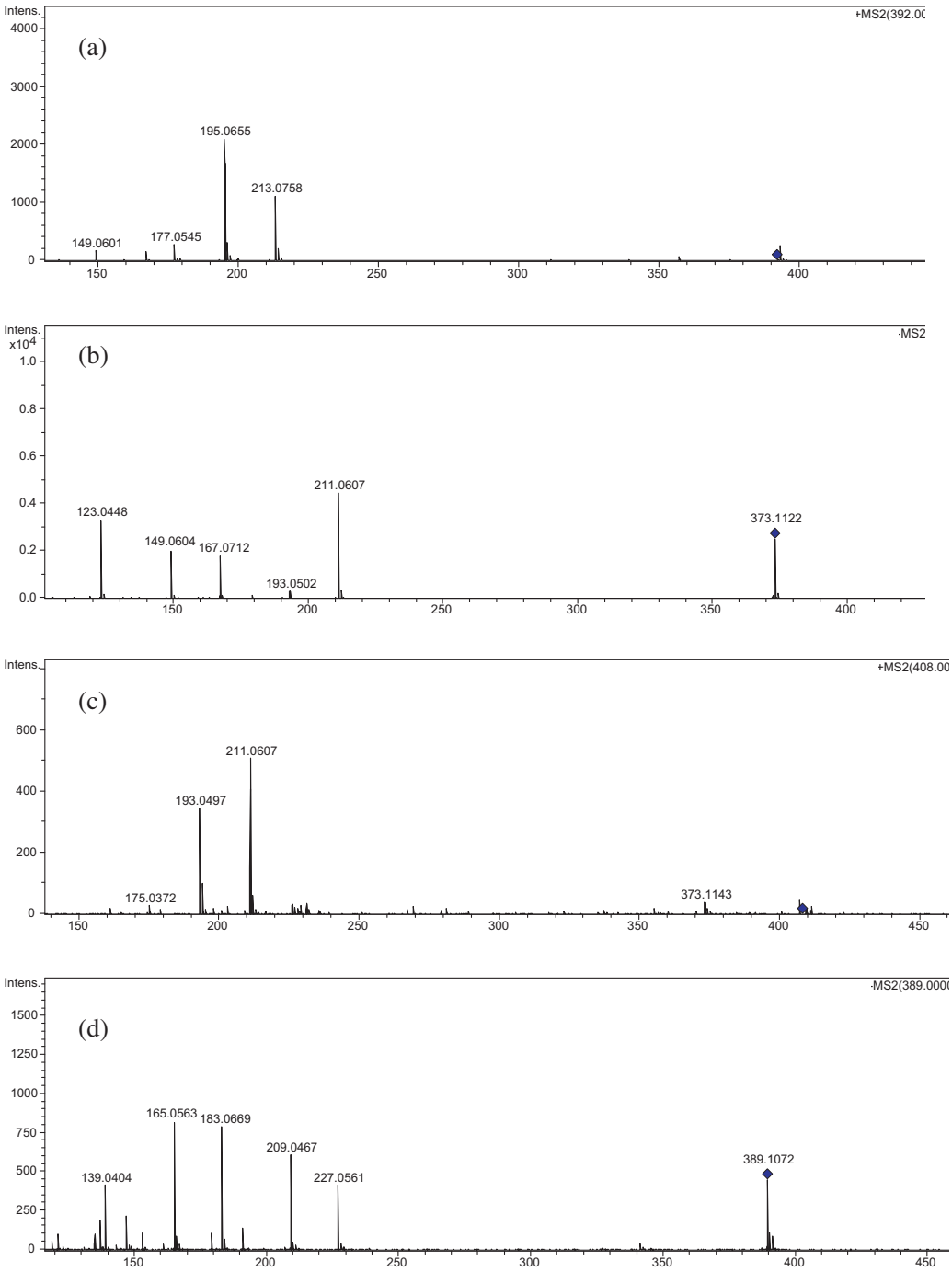

Fig. 3. Product ion scan of the selected precursor: (a) $[M+NH_4]^+$ at *m/z* 392 (collision energy: 8 eV) and (b) $[M-H]^-$ at *m/z* 373 for geniposidic acid (**8**) (collision energy: 17 eV); and (c) $[M+NH_4]^+$ at *m/z* 408 (collision energy: 8 eV) and (d) $[M-H]^-$ at *m/z* 463 for deacetylasperulosidic acid (**9**) (collision energy: 17 eV).

m/z 211 by loss of Glc. Compound **9** may be deacetylasperulosidic acid. In negative ion mode, the MS/MS spectrum of [M−H]–at *m/z* 389 (Fig. 3d) was similar to that of **1** and **3**, implying the structure proposed in Fig. 1.

Compound **10** was tentatively identified as decatylasperuloside acid methyl ester based on the accurate mass of $[M+NH_4]^+$ at *m/z* 422.1659 and the tandem MS spectrum in positive ion mode. The loss of a CH_3OH molecule from each of the product ions at *m/z* 405 and 243, indicated that the carboxyl might be methylated. The formula of compound **11** is $C_{16}H_{22}O_{12}$, based on the accurate mass of $[M+NH_4]^+$ at *m/z* 424.1466. The possible structure of **11** is shown in Fig. 1. The product ion at *m/z* 245 was formed from *m/z* 424 by loss of NH_3 and Glc, and further yielded the product ions at *m/z* 227 and 209 by loss of a H_2O molecule.

3.4. Structural analysis of compounds 12–15 with phenolic acid groups

Compounds **12**–**15** may have phenolic acid groups (Fig. 1). The molecular formula of compound **14** was identified as $C_{25}H_{28}O_{14}$ based on the accurate mass of the $[M+NH_4]^+$ ion at *m/z* 570.1807 and RIA measurements (Table 1). The skeleton structure of compound **14** was the same as **1**, based on their comparative MS/MS spectra in positive ion mode (Fig. 4 and Supporting Information).

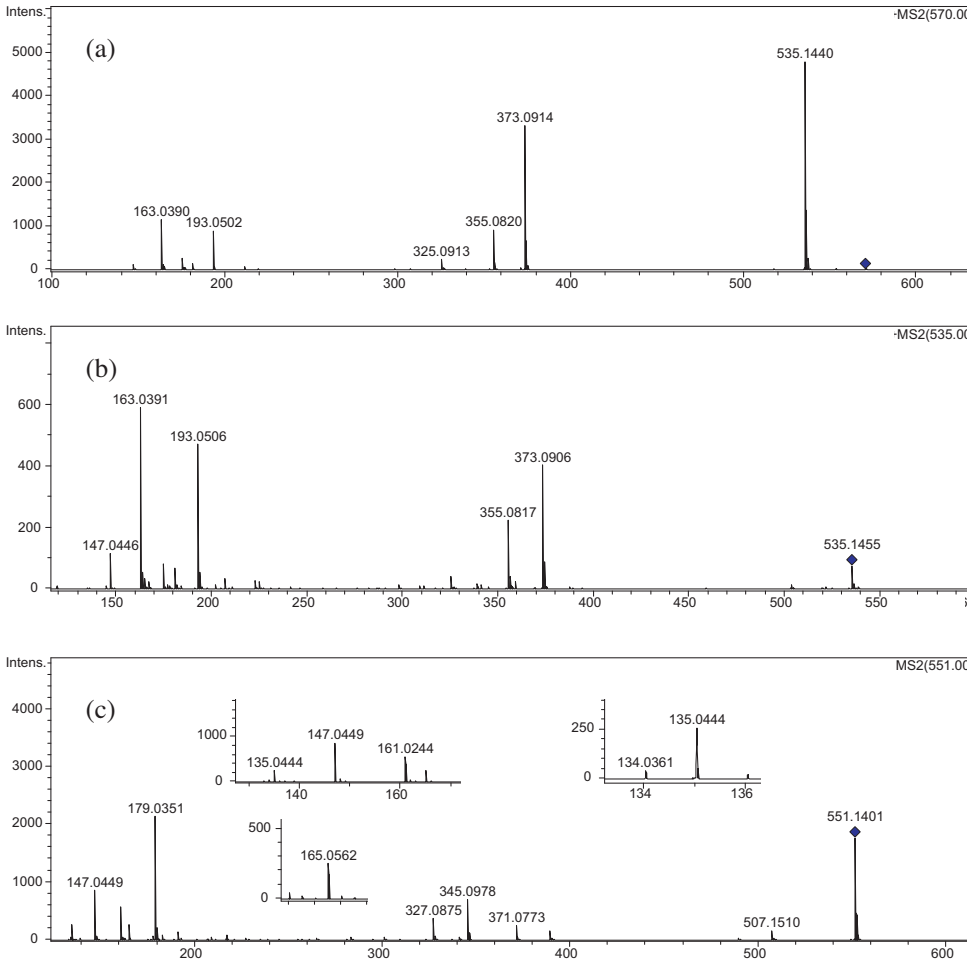

Fig. 4. MS/MS and MS/MS/MS spectra for compound **14**: (a) selected precursor $[M+NH_4]^+$ at *m*/*z* 570 (collision energy: 8 eV); (b) selected ion at *m*/*z* 535 from *m*/*z* 570 (collision energy: 8 eV); and selected precursor $[M-H]^-$ at *m*/*z* 551(collision energy: 23 eV).

The neutral loss of $C_9H_8O_4$ from the product ion at *m*/*z* 373 was observed. The product ions at *m*/*z* 181 and 163 were likely to have been derived from the side chain group on the iridoid moiety. In negative ion mode, the losses of Glc, H_2O, and CO_2 were the main neutral losses. Notably, the product ions at *m*/*z* 181 and 163 in positive ion mode and the product ions at *m*/*z* 179, 161, 135 and 134 in negative ion mode (Tables 2 and 3) are the characteristic ions of caffeic acid [20]. The detailed fragmentation pathways of *m*/*z* 570 in positive-ion mode and *m*/*z* 551 in negative ion mode for compound **14** are shown in Scheme 1. The structure of compound **13** was very similar to that of **14**. The high-abundance product ion at *m*/*z* 147 in positive ion mode and the product ions at *m*/*z* 163, 145 and 119 in negative ion mode, indicated that the coumaric acid in **13** substitutes caffeic acid in **14** (Fig. 1).

The molecular formula of compound **15** is $C_{26}H_{30}O_{14}$, which represents a difference of CH_2 from molecular formulas of **14**, and indicates that an H atom might be substituted by a methyl group. The product ions at *m*/*z* 195, 177, 163, and 145 from the $[M+NH_4]^+$ ion at *m*/*z* 584 in positive ion mode (Fig. 5), and the product ions at *m*/*z* 193, 175, and 161 from $[M-H]^-$ at *m*/*z* 565 in negative ion mode (Fig. 5 and Table 4) further imply that the caffeic acid moiety in **15** is methylated. The high abundance product ion at *m*/*z* 339 in positive ion mode was formed by losses of NH_3 and iridoid moiety from *m*/*z* 584, which indicates that the methylated caffeic acid moiety is directly linked to a sugar. The product ions at *m*/*z* 337, which in negative ion mode resulted from *m*/*z* 565 by loss of the iridoid moiety, provided three characteristic ions at *m*/*z* 295, 265, and 235, through cleavage of the sugar moiety (Scheme 2). The three ions suggested that the methylated caffeic acid moiety

Table 2
Elemental constituents of major product ions from $[M+NH_4]^+$ for compound (**14**).

Ion	Formula	Calculated	Observed	Error (ppm)
$[M+NH_4]^+$	$C_{25}H_{32}NO_{14}$	570.1817	–	–
$[M+NH_4-NH_3-H_2O]^+$	$C_{25}H_{27}O_{13}$	535.1446	535.1455	−1.7
$[M+NH_4-NH_3-H_2O-C_6H_{10}O_5]^+$	$C_{19}H_{17}O_8$	373.0918	373.0906	3.2
$[M+NH_4-NH_3-H_2O-C_6H_{12}O_6]^+$	$C_{19}H_{15}O_7$	355.0812	355.0817	−1.4
$[M+NH_4-NH_3-H_2O-C_6H_{10}O_5-C_9H_8O_4]^+$	$C_{10}H_9O_4$	193.0495	193.0506	−0.5
$[Caffeic\ acid+H]^+$	$C_9H_9O_4$	181.0495	181.0497	−1.1
$[M+NH_4-NH_3-H_2O-C_6H_{12}O_6-C_9H_8O_4]^+$	$C_{10}H_7O_3$	175.0390	175.0390	0.1
$[Caffeic\ acid+H-H_2O]^+$	$C_9H_7O_3$	163.0390	163.0390	0.0
$[C_9H_7O_2]^+$	$C_9H_7O_2$	147.0441	147.0449	−5.4

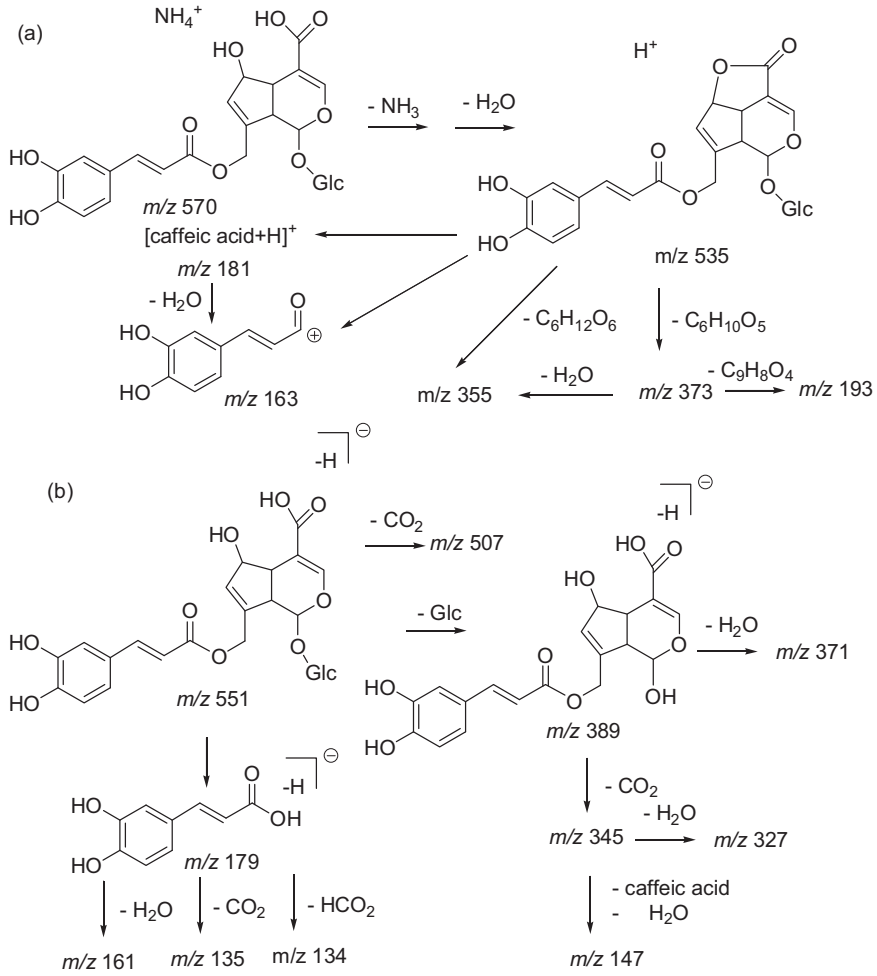

Scheme 1. Major fragmentation pathways of (a) $[M+NH_4]^+$ and (b) $[M-H]^-$ for compound **14**.

Table 3
Elemental constituents of major product ions from $[M-H]^-$ for compound (**14**).

Ion	Formula	Calculated	Observed	Error (ppm)
$[M-H]^-$	$C_{25}H_{27}O_{14}$	551.1406	551.1401	0.9
$[M-H-CO_2]^-$	$C_{24}H_{27}O_{12}$	507.1508	507.1501	1.4
$[M-H-C_6H_{10}O_5]^-$	$C_{19}H_{17}O_9$	389.0878	389.0900	−5.7
$[M-H-C_6H_{12}O_6]^-$	$C_{19}H_{15}O_8$	371.0772	371.0773	−0.3
$[M-H-C_6H_{10}O_5-CO_2]^-$	$C_{18}H_{17}O_7$	345.0974	345.0978	−1.2
$[M-H-C_6H_{12}O_6-CO_2]^-$	$C_{18}H_{15}O_6$	327.0874	327.0875	−0.3
[Caffeic acid–H]$^-$	$C_9H_7O_4$	179.0350	179.0351	−0.6
$[M-H-C_6H_{10}O_5-CO_2-C_9H_8O_4]^-$	$C_9H_9O_3$	165.0557	165.0562	−3.0
[Caffeic acid–H–H_2O]$^-$	$C_9H_5O_3$	161.0244	161.0244	0.1
$[M-H-C_6H_{10}O_5-CO_2$–caffeic acid–$H_2O]^-$	$C_9H_7O_2$	147.0452	147.0449	2.0
[Caffeic acid–H–CO_2]$^-$	$C_8H_7O_2$	135.0452	135.0444	5.9
[Caffeic acid–H–HCO_2]$^-$·	$C_8H_6O_2$	134.0373	134.0361	8.9

is directly linked to the 6-OH group of the sugar. We previously reported a very similar fragmentation pattern [20]. The structure of compound **12** appears to be similar to that of **15**, and comprise iridoid, pentose and caffeic acid moieties (Fig. 1).

3.5. Structural analysis of compounds 16–18 with two sugar groups

Compounds **16**–**18** appeared to contain two sugar groups. For compound **16** the accurate mass of the $[M+NH_4]^+$ ion at *m*/*z* 644.1858 provided the molecular formula $C_{24}H_{34}O_{17}S$, and the product ions at *m*/*z* 447, 285, 267, 193, and 175 in MS/MS spectrum in positive ion mode were the same as for **1** (see Supporting Information), implying that compound **16** includes the same structural moieties as **1**. The product ion at *m*/*z* 609, which was derived from *m*/*z* 644 thorough the loss of NH_3 and H_2O molecules, further produced the product ion at *m*/*z* 447 by loss of $C_6H_{10}O_5$, which indicate the hexose. MS/MS spectra indicated that compound **17** may contain the structure of **3**. It was also deduced that another moiety in **17** was hexose based on the neutral loss of $C_6H_{10}O_5$ from *m*/*z* 612. Based on MS/MS spectra (Supporting Information), compound **18** contains the moieties of **13** and pentose.

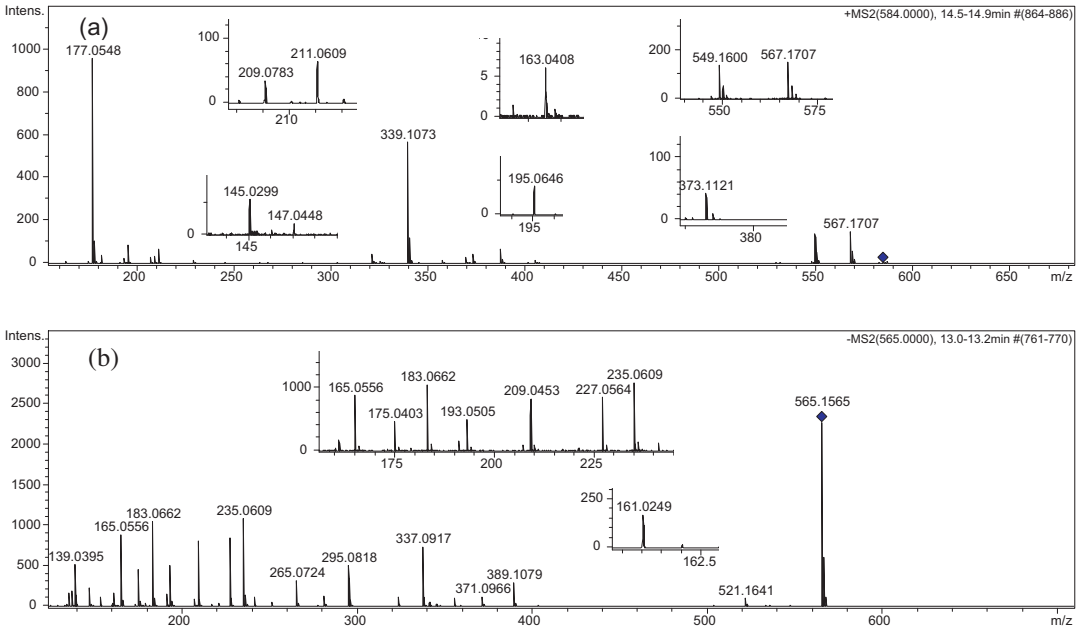

Fig. 5. Product ion scan of the selected precursor for compound **15**: (a) $[M+NH_4]^+$ at *m/z* 584 (collision energy: 8 eV); and (b) $[M-H]^-$ at *m/z* 565 (collision energy: 23 eV).

Table 4
Elemental constituents of major product ions from $[M-H]^-$ for compound (**15**).

Ion	Formula	Calculated	Observed	Error (ppm)
$[M-H]^-$	$C_{26}H_{29}O_{14}$	565.1563	565.1565	−0.3
$[M-H-CO_2]^-$	$C_{25}H_{29}O_{12}$	521.1664	521.1641	4.4
$[M-H-C_{10}H_8O_3]^-$	$C_{16}H_{21}O_{11}$	389.1089	389.1079	3.0
$[M-H-C_{10}H_8O_3-H_2O]^-$	$C_{16}H_{19}O_{10}$	371.0984	371.0966	−4.9
$[M-H-C_{10}H_{12}O_6(\text{iridoid})]^-$	$C_{16}H_{17}O_8$	337.0929	337.0917	3.6
$[M-H-C_{10}H_{12}O_6(\text{iridoid})-C_2H_2O]^-$ (cleavage of sugar)	$C_{14}H_{15}O_7$	295.0823	295.0818	1.7
$[M-H-C_{10}H_{12}O_6(\text{iridoid})-C_3H_4O_2]^-$ (cleavage of sugar)	$C_{13}H_{13}O_6$	265.0718	265.0724	−1.9
$[M-H-C_{10}H_{12}O_6(\text{iridoid})-C_4H_6O_3]^-$ (cleavage of sugar)	$C_{12}H_{11}O_5$	235.0612	235.0609	1.3
$[M-H-C_{10}H_8O_3-C_6H_{10}O_5]^-$	$C_{10}H_{11}O_6$	227.0561	227.0564	−1.3
$[M-H-C_{10}H_8O_3-C_6H_{12}O_6]^-$	$C_{10}H_9O_5$	209.0455	209.0453	1.0
$[\text{Phenolic acid}-H]^-$	$C_{10}H_9O_4$	193.0506	193.0505	0.5
$[M-H-C_{10}H_8O_3-C_6H_{10}O_5-CO_2]^-$	$C_9H_{11}O_4$	183.0663	183.0662	0.5
$[\text{Phenolic acid}-H-H_2O]^-$	$C_{10}H_7O_3$	175.0401	175.0403	−1.1
$[\text{Caffeic acid}-H-\text{MeOH}]^-$	$C_9H_5O_3$	161.0244	161.0249	−3.1

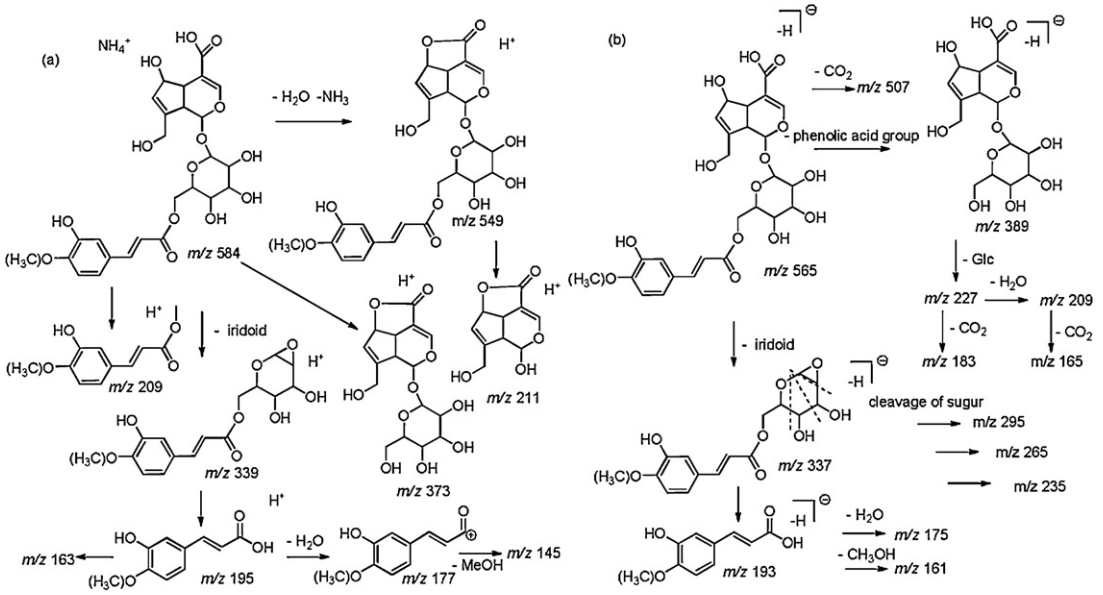

Scheme 2. Major fragmentation pathways of (a) $[M+NH_4]^+$ and (b) $[M-H]^-$ for compound **15**.

Table 5
Elemental constituents of major product ions from $[M+NH_4]^+$ for compound (**19**).

Ion	Formula	Calculated	Observed	Error(ppm)
$[M+NH_4]^+$	$C_{36}H_{48}NO_{22}S_2$	910.2104	910.2119	−1.6
$[M+NH_4-NH_3-H_2O]^+$	$C_{36}H_{43}O_{21}S_2$	875.1733	875.1760	−3.1
$[M+NH_4-NH_3-H_2O-C_6H_{10}O_5]^+$	$C_{30}H_{33}O_{16}S_2$	713.1205	713.1231	−3.6
$[M+NH_4-NH_3-H_2O-C_6H_{10}O_5-H_2O-CH_3SCOOH]^+$	$C_{28}H_{27}O_{13}S$	603.1167	603.1170	−0.5
$[M+NH_4-NH_3-H_2O-C_{12}H_{12}O_6S]^+$	$C_{24}H_{31}O_{15}S$	591.1378	591.1387	−1.5
$[713-C_{12}H_{12}O_6S]^+$ or $[M+NH_4-NH_3-C_{18}H_{24}O_{12}S]^+$	$C_{18}H_{21}O_{10}S$	429.0850	429.0837	3.0
$[429-CH_3SCOOH]^+$	$C_{16}H_{17}O_8$	337.0918	337.0915	0.9
$[429-CH_3SCOOH-H_2O]^+$	$C_{16}H_{15}O_7$	319.0812	319.0813	−0.3
$[C_{12}H_{12}O_6S+H]^+$	$C_{12}H_{13}O_6S$	285.0427	285.0425	0.7
$[C_{12}H_{10}O_5S+H]^+$	$C_{12}H_{11}O_5S$	267.0322	267.0325	−1.1
$[C_{10}H_8O_4+H]^+$	$C_{10}H_9O_4$	193.0495	193.0498	−1.6
$[C_{10}H_6O_3+H]^+$	$C_{10}H_7O_3$	175.0390	175.0389	0.6

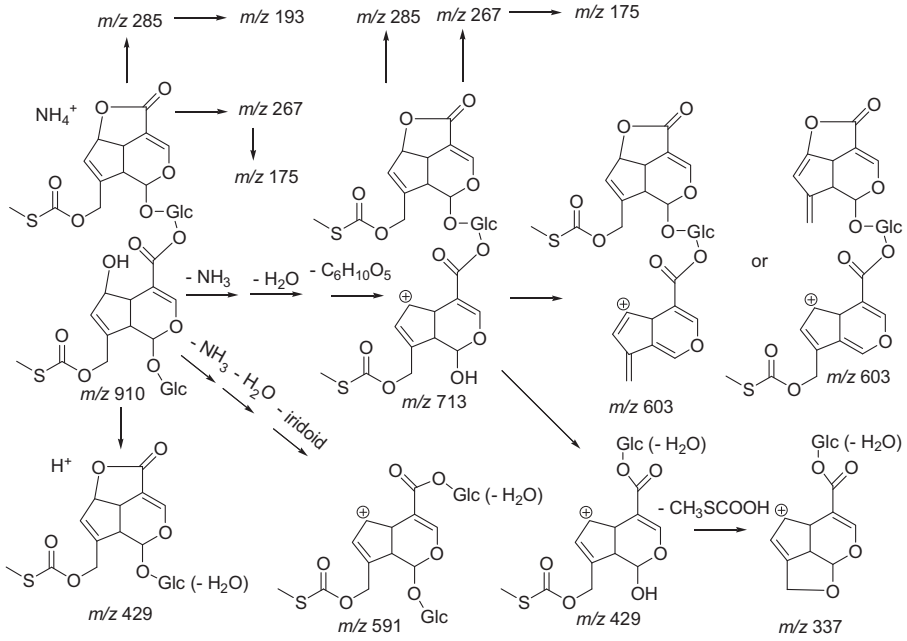

Scheme 3. Major fragmentation pathways of $[M+NH_4]^+$ for compound **19**.

3.6. Structural analysis of iridoid glucoside dimers 19–24

Compounds **19**–**24** are dimeric iridoid glucosides. For compound **19** the accurate mass of the $[M+NH_4]^+$ ions at *m/z* 910.2117and RIA measurements gave the molecular formula $C_{36}H_{44}O_{22}S_2$. This, and the product ions at *m/z* 285, 267, 193 and 175 in the MS/MS spectrum (Table 5 and supporting information) indicate that **19** may be a dimeric paederoside. Cleavage of the glycosidic bond and the loss of H_2O and CH_3SCOOH were the main fragmentation patterns for **19** (Scheme 3). The product ion at *m/z* 591 was the characteristic ion. A labeling experiment involving H/D exchange in **19** was carried out (the MS/MS spectrum is shown in Supporting Information). The product ion at *m/z* 597 indicated six active H atoms, which provided further support for the structure of the characteristic ion. The accurate mass, RIA measurements, and MS/MS spectra of compound **20** imply that it is an isomer of **19**. The product ions of compounds **19** and **20** were the same, but their relative abundances varied greatly. Except for *m/z* 603, the relative abundances of the product ions were much lower for **20** than for **19**. This suggests that the difference between the two compounds is the linkages between the carboxyl group and the hydroxyl groups on the sugar.

Compound **21** has the molecular formula $C_{36}H_{44}O_{22}S$, and comprises compounds **2** and **4**. The product ions at *m/z* 285, 267, 253, 235, 193, and 175 in the MS/MS spectrum (Fig. 6) implied that **21** is a dimeric iridoid glucosides of paederoside (**2**) and asperuloside (**4**) (Fig. 1 and Scheme 4). The characteristic product ion at *m/z* 559 indicates that the carboxyl group of asperuloside (**4**) is linked to the hydroxyl groups on the sugar of paederoside (**2**). The product ion at *m/z* 565 in the D-labeling spectrum supported this analysis (Fig. 6). Compound **22** is an isomer of **21**, based on their molecular formulae and MS/MS spectra. The characteristic product ion at *m/z* 591 implies that the carboxyl of asperuloside (**2**) is connected to the hydroxyl groups on the sugar of paederoside (**4**) (Fig. 1). Relative to **21**, the MS/MS spectrum of **22** showed that the product ion at *m/z* 571, 429, 253 and 235 were in high abundance, but at *m/z* 397, 285, and 267 the product ion was in low abundance. These product ions are the characteristic ions for determinating the connection order between the asperuloside (**2**) and paederoside (**4**) parts of the dimeric iridoid glucosides (Fig. 1). In addition, for **21** the greater relative abundance of the product ion at *m/z* 603 than that at *m/z* 571 and the opposite relationship for **22,** provides additional information for determinating the connection order. However, the connections are difficult to be confirmed even with the use of NMR spectroscopy. Because the ^1H and ^{13}C-NMR spectra can overlap and reduce the quality of the (^1H-detected) heteronuclear multiple-bond correlation (HMBC) spectra.

Compounds **21**, **22**, **23** and **24** are isomers. As with the MS/MS spectrum of compound **20**, the relative abundance of many product ions was very low for **23** and **24**. Despite this, the connection order

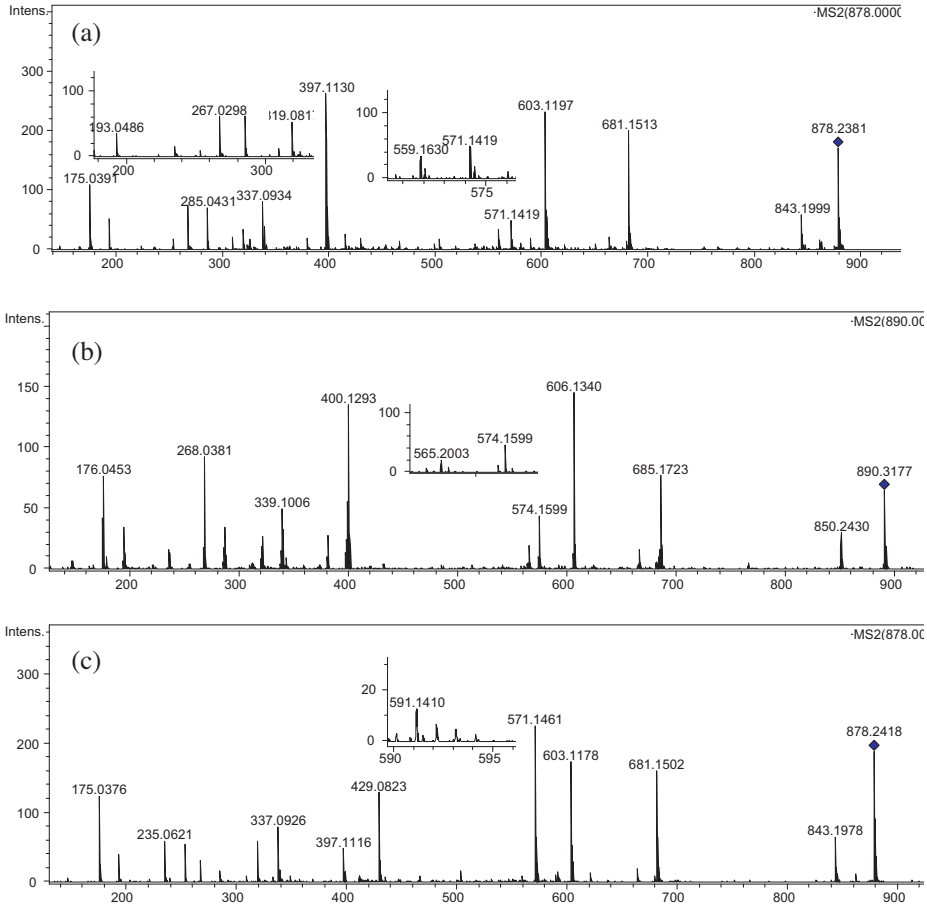

Fig. 6. Product ion scan of the selected precursor: (a) $[M+NH_4]^+$ at *m/z* 878 (collision energy: 10 eV) and (b) deuterated precursor ion at *m/z* 890 (collision energy: 10 eV) for compound **21**; and (c) $[M+NH_4]^+$ at *m/z* 878 (collision energy: 10 eV) for compound **22** (collision energy: 10 eV).

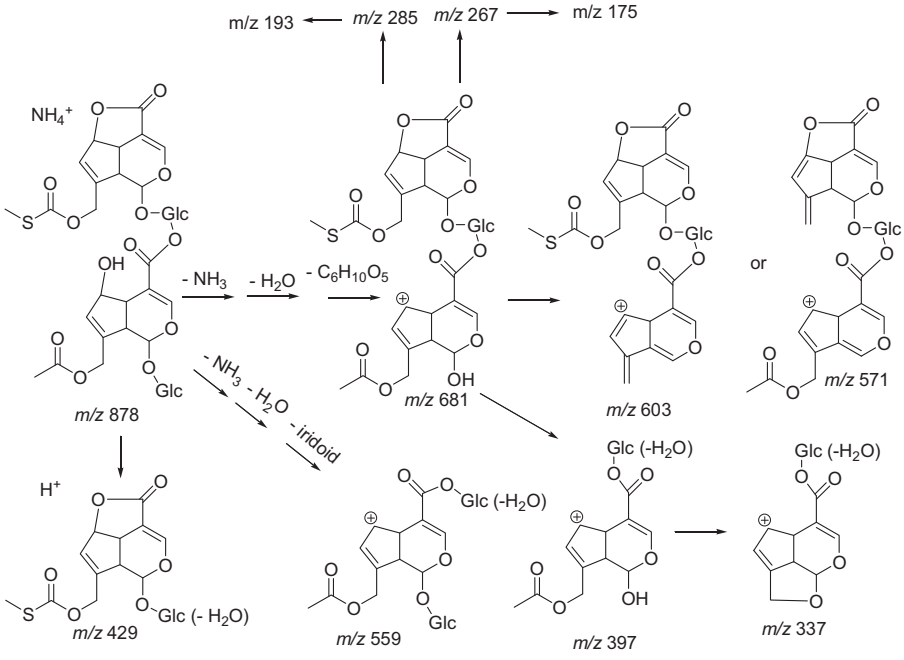

Scheme 4. Major fragmentation pathways of $[M+NH_4]^+$ for compound **21**.

between the asperuloside (**2**) and paederoside (**4**) parts of **23** and **24** was confirmed by comparison of the MS/MS spectra of **21**, **22**, **23** and **24** (Fig. 6 and Supporting Information).

4. Conclusion

A series of iridoid glucosides in an extract of *P. scandens* was investigated using HPLC–ESI-QTOF, without the use of standard samples. A total of 24 (including 14 possibly new) iridoid glucosides were identified or tentatively characterized based on exact masses, RIA values, tandem mass spectra, D-labeling experiments, and previously reported data. A number of complex compounds were identified that contained a phenolic acid group in combination with iridoid and sugar moieties. Acylation of the 6-OH group of the sugar by phenolic acid was detected, and the connection order between the asperuloside and paederoside moieties in the dimeric iridoid glucosides was confirmed by the characteristic product ions; such analyses are very challenging, even those based on NMR.

Although the structure of compounds could not be fully confirmed using only MS, HPLC–ESI-QTOF-MS/MS proved to be a powerful tool for compound identification, especially for trace natural products in a complex mixture. MS can provide important structural information that cannot be obtained by NMR. The comprehensive component analysis, especially with respect to trace compounds in plant extracts will be useful in understanding the diversity of plant metabolic diversity and biosynthetic processes.

Acknowledgments

This study was funded by the Chinese Academy of Sciences (CAS) for Development and Innovation of Apparatus (YG2010078) and by the CAS Frontier Fields of Knowledge Innovation Project.

Appendix A. Supplementary data

Supplementary data associated with this article can be found, in the online version, at http://dx.doi.org/10.1016/j.jchromb.2013.01.032.

References

[1] D.N. Quang, T. Hashimoto, M. Tanaka, N.X. Dung, Y. Asakawa, Iridoid glucosides from roots of Vietnamese *Paederia scandens*, Phytochemistry 60 (2002) 505.
[2] G.J. Kapadia, S.C. Sharma, H. Tokuda, H. Nishino, S. Ueda, Inhibitory of iridoid glucosides on Epstein–Barr virus activation by short-term in vitro assay for anti-tumor promoters, Cancer Lett. 102 (1999) 223.
[3] N.N. Tran, Gop phan vao viec thong ke nhung loai thuc vat co ich thuoc ho ca phe (Rubiaceae Juss) o Vietnam (Contribution to the enumeration of useful species of the family Rubiaceae juss in Vietnam), J. Biol. 9 (1987) 40.
[4] H. Inouye, S. Inouye, N. Shimokawa, M. Okigawa, Studies on monoterpene glucosides. VII. Iridoid glucosides of *Paederia scandens*, Chem. Pharm. Bull. 17 (1969) 1942.
[5] H. Inouye, M. Okigawa, N. Shimokawa, Studies on monoterpene glucosides. VIII. Artifacts formed during extraction of asperuloside and paederoside, Chem. Pharm. Bull. 17 (1969) 1949.
[6] G.J. Kapadia, Y.N. Shukla, A.K. Bose, H. Fujiwara, H.A. Lloyd, Revised structure of paederoside, a novel monoterpene S-methyl thiocarbonate, Tetrahedron Lett. 22 (1979) 1937.
[7] Y.L. Kim, Y.W. Chin, J. Kim, J.H. Park, Two new acylated iridoid glucosides from the aerial parts of *Paederia scandens*, Chem. Pharm. Bull. 52 (2004) 1356.
[8] X. Zuo, S. Peng, X. Liu, B. Bai, L.S. Ding, Sulfur-containing iridoid glucosides from *Paederia scandens*, Fitoterapia 77 (2006) 374.
[9] H. Otsuka, Two new iridoid glucosides in Paederia scandens (Lour.) Merr. Var. mairei (Leveille) Hara, Nat. Med. (Tokyo) 56 (2002) 59.
[10] Y.C. Wang, T.L. Huang, Screening of anti-helicobacter pylori herbs deriving from Taiwanese folk medicinal plants, FEMS Immunol. Med. Microbiol. 43 (2005) 295.
[11] T. Konoshima, M. Takasaki, H. Tokuda, N. Hoyoku, Cancer chemopreventive activity of an iridoid glycoside, 8-acetylharpagide, from *Ajuga decumbens*, Cancer Lett. 157 (2000) 87.
[12] Y.F. Chen, N. Li, Y.L. Jiao, P. Wei, Q.Y. Zhang, K. Rahman, H.C. Zheng, L.P. Qin, Antinociceptive activity of petroleum ether fraction from the MeOH extracts of *Paederia scandens* in mice, Phytomedicine 15 (2008) 427.
[13] J.J. Karchesy, R.W. Hemingway, Y.L. Foo, E. Barofsky, D.F. Barofsky, Sequencing procyanidin oligomers by fast atom bombardment mass spectrometry, Anal. Chem. 58 (1986) 2563.
[14] H.J. Li, M.L. Deinzer, Tandem mass spectrometry for sequencing proanthocyanidins, Anal. Chem. 79 (2007) 1739.
[15] Z.J. Wu, G.Y. Li, D.M. Fang, H.Y. Qi, W.J. Ren, G.L. Zhang, Analysis of epipolythiodioxopiperazines in fungus Chaetomium cochliodes using HPLC–ESI-MS/MS/MS, Anal. Chem. 80 (2008) 217.
[16] N. Es-Safi, L. Kerhoas, P.H. Ducrot, Fragmentation study of iridoid glucosides through positive and negative electrospray ionization, collision-induced dissociation and tandem mass spectrometry, Rapid Commun. Mass Spectrom. 21 (2007) 1165.
[17] L.L. Ren, X.Y. Xue, F.F. Zhang, Y.C. Wang, Y.F. Liu, C.M. Li, X.M. Liang, Studies of iridoid glycosides using liquid chromatography/electrospray ionization tandem mass spectrometry, Rapid Commun. Mass Spectrom. 21 (2007) 3039.
[18] C.M. Li, X.L. Zhang, X.Y. Xue, F.F. Zhang, Q. Xu, X.M. Liang, Structural characterization of iridoid glucosides by ultra-performance liquid chromatography/electrospray ionization quadrupole time-of-flight tandem mass spectrometry, Rapid Commun. Mass Spectrom. 22 (2008) 1941.
[19] Y. Zhou, X. Zou, X. Liu, S.L. Peng, L.S. Ding, Multistage electrospray ionization mass spectrometric analyses of sulfur-containing iridoid glucosides in *Paederia scandens*, Rapid Commun. Mass Spectrom. 21 (2007) 1375.
[20] Z.J. Wu, X.L. Ma, D.M. Fang, H.Y. Qi, W.J. Ren, G.L. Zhang, Analysis of caffeic acid derivatives from *Osmanthus yunnanensis* using electrospray ionization quadrupole time-of-flight tandem mass spectrometry, Eur. J. Mass Spectrom. 15 (2009) 415.